Pergamon

Geochimica et Cosmochimica Acta, Vol. 66, No. 16, pp. 2903–2913, 2002

0016-7037/02 $22.00 + .00

PII S0016-7037(00)00875-X

Diffusion kinetics of Fe^{2+} and Mg in aluminous spinel: Experimental determination and applications

HANNS-PETER LIERMANN[1] and JIBAMITRA GANGULY
Department of Geosciences, University of Arizona, Tucson, AZ 85721, USA

(*Received August* 22, 2001; *accepted in revised form February* 19, 2002)

Abstract—The diffusion coefficients of Fe^{2+} and Mg in aluminous spinel at ~20 kb, 950 to 1325°C, and at 30 kb, 1125°C have been determined via diffusion couple experiments and numerical modeling of the induced diffusion profiles. The oxygen fugacity, fO_2, was constrained by graphite encapsulating materials. The retrieved self-diffusion coefficients of Fe^{2+} and Mg at ~20 kb, 950 to 1325°C, fit well the Arrhenian relation, $D = D_0\exp(-Q/RT)$, where Q is the activation energy, with $D_0(Fe) = 1.8\ (\pm 2.8) \times 10^{-5}$, $D_0(Mg) = 1.9\ (\pm 1.4) \times 10^{-5}$ cm^2/s, $Q(Fe) = 198 \pm 19$, and $Q(Mg) = 202 \pm 8$ kJ/mol. Comparison with the data at 30 kb suggests an activation volume of ~5 cm^3/mol. From analysis of compositional zoning in natural olivine-spinel assemblages in ultramafic rocks, previous reports concluded that D(Fe-Mg) in spinel with $Cr/(Cr + Al) \leq 0.5$ is ~10 times that in olivine. The diffusion data in spinel and olivine have been applied to the problems of preservation of Mg isotopic inhomogeneity in spinel within the plagioclase–olivine inclusions in Allende meteorite and cooling rates of terrestrial ultramafic rocks. *Copyright © 2002 Elsevier Science Ltd*

1. INTRODUCTION

Diffusion data in spinel are of interest in a number of terrestrial and planetary problems. Ozawa (1984) attempted to constrain the cooling rates of ultramafic rocks (peridotites, gabbros, picrites) on the basis of diffusion kinetic modeling of compositional gradients in coexisting spinel and olivine. Sheng et al. (1992) used the diffusion kinetic constraint on the preservation of isotopic heterogeneity of Mg in spinel to deduce heating and initial cooling rate of the plagioclase–olivine inclusions (POIs) in the Allende meteorite. The interdiffusion of Fe^{2+} and Mg also seems to play a critical role in the oxidation or "maghematization" process of spinel in seafloor basalts and therefore in the interpretation of their paleomagnetic record (Freer and O'Reilly, 1980).

Freer and O'Reilly (1980) determined the Fe^{2+}-Mg interdiffusion coefficient, D(Fe-Mg), in spinel as a function of temperature (800 to 1034°C) and composition using sintered pellets of synthetic spinels of different compositions. Their data show a strong compositional dependence of D(Fe-Mg), which increases with decreasing Fe^{2+} content in spinel. Sheng et al. (1992) determined Mg self-diffusion coefficient, D(Mg), in a nearly pure natural $MgAl_2O_4$-spinel (MgO: 28.2, Al_2O_3: 72.63, SiO_2: 0.03, CaO: 0.02 wt%) at 1261 to 1553°C by using diffusion couples consisting of Mg isotope–enriched melt, which was in bulk chemical equilibrium with the spinel. The extrapolated D(Mg) value at ~1000°C is more than four orders of magnitude smaller than D(Fe) value that is constrained by the interdiffusion data of Freer and O'Reilly (1980) according to the relation that $D(i - j) = D(i)$ as $X_i \rightarrow 0$ (e.g., Manning, 1968). Although not impossible, such a large difference between D(Fe) and D(Mg) is surprising, in view of the available data on the self-diffusion coefficients in garnet (Chakraborty and Ganguly, 1992; Ganguly et al., 1998a) and the difference between the D(Mg) and D(Fe-Mg) at $X_{Mg} = 0.86$ in olivine (Chakraborty, 1997). Furthermore, the diffusion profiles shown by Freer and O'Reilly (1980) are irregular, which makes one suspect that their experiments were probably marred by interference from grain boundary diffusion.

On the other hand, the Mg self-diffusion data, D(Mg), of Sheng et al. (1992) are not adequate for modeling the diffusion induced modification of Fe-Mg compositional zoning in spinel. For the latter purpose, one needs the interdiffusion data as a function of composition or self-diffusion data of both Fe^{2+} and Mg from which the D(Fe-Mg) may be calculated at any composition in the binary system. In addition, the point defect chemistry, and hence the diffusion properties of iron-bearing samples, could be quite different from those in samples that are essentially free of iron (Chakraborty et al., 1994), such as the ones used by Sheng et al. (1992).

We have undertaken a systematic study of the cation diffusion kinetics in spinel that would eventually lead to an improved understanding of the thermal histories of terrestrial and planetary samples. In this work, we report the results of diffusion couple experiments in the Fe-Mg binary system at 950 to 1325°C and their applications to constrain the D(Fe-Mg) data in olivine, which have been controversial, and to the cooling rates of selected terrestrial ultramafic rocks and the POIs in Allende meteorite.

2. EXPERIMENTAL STUDIES

Conventionally, a diffusion couple experiment involves the use of two gem-quality single crystals of the same mineral, but with contrasting compositions. These are assembled together with a highly polished interface and annealed at a desired pressure–temperature (P-T) condition for a length of time that is sufficient to induce measurable diffusion of the components of interest. The resulting diffusion profiles are then modeled to retrieve the self-diffusion coefficients of the components (e.g., Chakraborty and Ganguly, 1992; Ganguly et al., 1998a) or the interdiffusion coefficients in a binary system (e.g., Buening and Buseck, 1973; Misener, 1974; Chakraborty, 1997). However, although there are natural sources of gem-quality single crys-

tals of Mg-rich aluminous spinels, we were unable to find any supply of the Fe^{2+}-rich counterparts. Thus, we used diffusion couples made of single crystal of Mg-rich aluminous spinel and sintered pellet of synthetic Fe^{2+}-rich spinel, as described below. Sintered pellets were used earlier by Schmalzried and coworkers (e.g., Hermeling and Schmalzried, 1984; Nakamura and Schmalzried, 1984) to measure volume diffusion properties of olivine. Although it is always preferable to use diffusion couples made from single crystals, the success of the sintered pellet technique enables one to conduct diffusion couple experiments on compositions for which natural single crystals are difficult to find.

2.1. Starting Materials and Sample Preparation

We used gem-quality octahedra of nearly pure Mg spinel from Sri Lanka. The single crystal had a composition of $(Mg_{0.99}Fe_{0.01})(Al_{1.997}Cr_{0.003})O_4$ (in wt%, MgO = 27.2 FeO = 0.41, Al_2O_3 = 70.84, Cr_2O_3 = 0.28). The sintered pellet of Fe^{2+}-rich spinel was prepared from mixtures of Fe_2O_3 (99.99%), MgO (99.998%), and γ-Al_2O_3 (>99.9%), where the parenthetical numbers indicate the purity levels. The oxides were mixed in appropriate proportions to yield aluminous spinel with 50 mol% Fe–end member component. The mixing procedure consisted of prolonged (~3 h) mixing in an agate mortar under alcohol with intermittent mixing in a mechanical shaker. The mixture was dried, enclosed in a graphite capsule, and subjected to a condition of 13 kb, 1150°C, for 48 h in a piston-cylinder apparatus. This procedure led to the reduction of Fe_2O_3 to FeO below the detection limit of Fe^{3+} by Mössbauer spectroscopy and to the in situ production of a sintered pellet. However, attempts to synthesize pure hercynite ($FeAl_2O_4$) according to the same procedure yielded spinel with Fe^{3+}/Fe(total) = 0.078, as determined by Mössbauer spectroscopy. Thus, we used only the intermediate spinels in the diffusion couple experiments. The individual crystals within the sintered pellets of synthetic spinel varied between 50 and 1000 μm in diameter. Although the compositions between different spinel crystals varied somewhat (~0.02 variation of X_{Fe}), the individual crystals were essentially homogeneous, as reflected by the compositional profiles determined by an electron microprobe.

For use as a microprobe standard, we synthesized hercynite from a stoichiometric mixture of FeO, which was produced from the reduction of 99.99% pure Fe_2O_3 and 99.99% pure Al_2O_3. The mixture was held within a BN capsule in a piston-cylinder apparatus at 13 kb, 1150°C, for 48 h. The product consisted predominantly of hercynite, along with some metallic iron and an iron–aluminum alloy. Because of the presence of metallic iron, no significant Fe^{3+} should be present in the synthetic hercynite. This was also confirmed by Mössbauer spectroscopy.

X-ray diffraction data of spinels used in the diffusion couple experiments were collected in a four-circle diffractometer. Refinement of the diffraction data yielded a = 8.0861(2) Å, V = 535.07(7) $Å^3$, and u = 0.2635(1) Å for the Mg-spinel, and a = 8.1183(4) Å, V = 535.05(7) $Å^3$ and u = 0.2629(4) Å for the intermediate spinel, where a, V, and u stand for the unit cell edge, unit cell volume, and oxygen positional parameter, respectively. Because Mg and Al have essentially the same X-ray scattering factors, the intracrystalline distribution of Mg and Al in the Mg-spinel could not be determined from the X-ray data. However, when compared with the calibration of u vs. the inversion parameter derived from neutron diffraction data (Redfern et al., 1999), the Mg-spinel seems to be completely ordered with all Mg in the tetrahedral sites and all Al in the octahedral sites. The structure refinement of the synthetic intermediate spinel also indicated that Fe^{2+} was confined completely to the tetrahedral sites.

One surface of each component (i.e., a natural Mg-spinel crystal and a sintered pellet of intermediate spinel) was polished stepwise with diamond pastes down to quarter-micron grit size. The surface of the single crystal was then finished to a mirror polish with a chemical-mechanical polishing with silica suspension on an OP-chem cloth (Struers). This procedure greatly reduces the surface damage that develops during purely mechanical polishing (Chakraborty and Rubie, 1996; Ganguly et al., 1998a). (The quality of the chemical-mechanical polishing depends on the rate of rotation of the polishing wheel, which in turn depends on the sample. For the spinel octahedra, best results were obtained at 1500 to 2000 turns/min.) However, chemical-mechanical polishing on the surface of sintered pellet caused partial disintegration of the grains as a result of preferential attack of the chemical agent to the grain boundaries. Thus, this final polishing step was abandoned for the sintered pellets.

To form a diffusion couple, the two components (i.e., single crystal and sintered pellet) were glued together at the polished surfaces and shaped into a cylinder. After removing the glue by dissolution in acetone, the components were thoroughly cleaned in an ultrasonic bath of acetone, dried, and reassembled to from a cylinder within a tightly fitting graphite capsule. The cylindrical geometry of the couple helps minimize its fracturing in the high P-T experiments in a piston-cylinder apparatus. A still better geometry is probably the conical one used by Elphick et al. (1985) and Chakraborty and Ganguly (1992), but the sample preparation according to this geometry is much more time-consuming. The cylindrical geometry seems to be a good compromise between machining time and the mechanical stability of the diffusion couple.

2.2. Diffusion-Couple Experiments

All diffusion experiments were conducted in an end-loaded piston-cylinder apparatus using a pressure vessel with a 3/4 inch internal diameter WC core, WC pistons, and talc-glass pressure cell with graphite internal resistance furnace. The pressure and temperature control systems were interfaced with a personal computer to record all data, including the power variation, during an experiment (see Bose and Ganguly, 1995, for details). The design of the pressure cell is illustrated in Figure 1. The initial distance between the thermocouple junction and the top surface of the diffusion couple was ~0.05 inches. Each pressure cell was wrapped within a thin (~0.001 inch) Pb foil and both the Pb foil and piston were painted on the outside with H-free MoS_2 lubricant (Molykote G-n paste from Dow-Corning) to reduce friction against the carbide core.

Temperature was measured by W-W3Re/W-W25Re thermocouples, which were encased in 99.99% pure alumina tubings. The thermocouple junction was embedded in ZrO_2 cement to

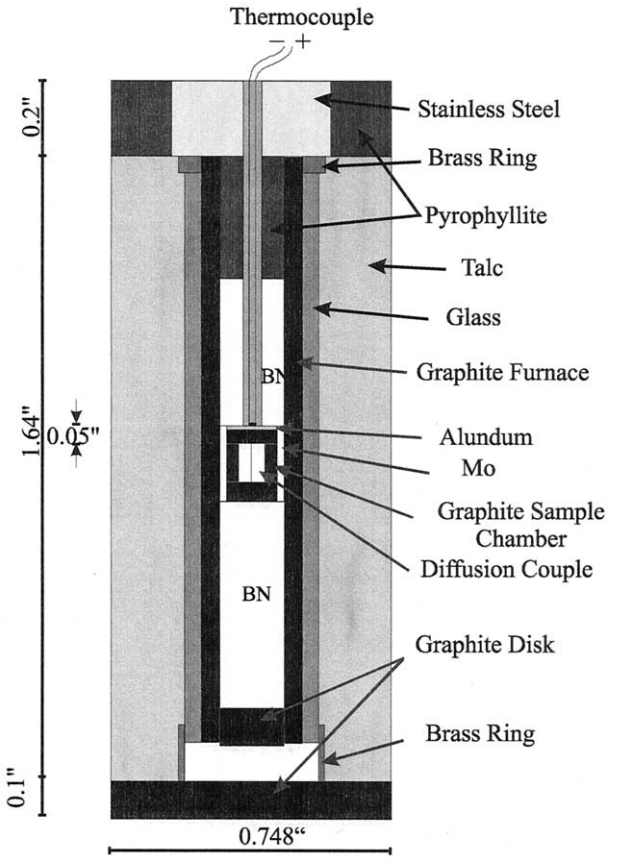

Fig. 1. Schematic cross section of talc-glass pressure cell used in diffusion couple experiments in piston-cylinder apparatus at high P-T conditions. The diffusion couple consisted of two half cylinders of nearly pure natural single crystal of $MgAl_2O_4$ spinel and sintered pellet of synthetic $(Fe_{0.5}Mg_{0.5})Al_2O_4$ spinel.

avoid contamination, and the emf was corrected with a cold junction correction integrated circuit (maximum error, 0.5%). Pressure effect on the emf of W/Re thermocouple is not known precisely. However, by using the analysis of Lane and Ganguly (1980), the error in temperature measurement in our studies due to the potential pressure effect was estimated to be within 5°C. The central horizontal section of the couple was made to coincide with that of the furnace. From previous experience with this type of pressure cells (Elphick et al., 1985), the temperature difference between the thermocouple tip and the top surface of the sample should have been within 5°C. As shown by Elphick et al. (1985), the metal ring surrounding the graphite sample holder serves to reduce the temperature gradient and prevent the ingress of pressure cell material, especially the molten glass, into the sample. The calibrated friction correction for the type of pressure cell used in this study is −10% of the nominal pressure (Chakraborty and Ganguly, 1992). Pressure was measured by both a 16-inch-diameter Heise gauge, calibrated to NBS standard, and an on-line digital pressure transducer.

Following the earlier practice in our laboratory, the sample was quenched gradually by stepwise reduction of temperature and pressure to avoid thermal shock and consequent fracturing of the diffusion couples. After pressing out of the pressure vessel, the pressure cell was immediately covered by a low-viscosity epoxy (Epo-Kwick by Buehler) that flowed into the cracks of the pressure cell. After curing the epoxy, the cell was thinned in a lathe and carefully sectioned to expose the top surface of the diffusion couple. The exposed surface of the sample was then covered with superglue to prevent fracturing due to possible release of residual stresses and polished normal to the interface for microprobe analysis. The diffusion experiments were carried out at six different temperatures between 950 and 1325°C, and except for two, all experiments were within ±1.5 kb of a mean nominal pressure of 21.2 kb. The experimental conditions are summarized in Table 1.

The oxygen fugacity, fO_2, is a potentially important variable in the study of diffusion kinetics of minerals containing elements that can occur in different valence states. In this study, fO_2 was constrained by the graphite encapsulating material. Chakraborty and Ganguly (1992) presented the fO_2 vs. T relations in the C-O-H system in the presence of graphite at 20 and 40 kbar, 1050 to 1500°C. In this system, the fO_2 is defined for a fixed value of H/O ratio. Chakraborty and Ganguly (1992) presented calculations for the limiting values of this ratio of 2 (i.e., C-H_2O system) and 0 (i.e., C-O_2 system). The fO_2 in the C-H_2O system is approximately a factor of 10 lower than that in C-O_2 system. These calculations can be used, by smooth graphical extrapolation to 950°C to determine the limiting fO_2 values prevailing in the present experimental studies. Because our sample assemblies were carefully dried before the experiments, the prevailing fO_2 in the diffusion couple experiments should have been very close to, but probably slightly lower than (because of the possible presence of small amount of hydrogen), that defined by the C(graphite)-O_2 system. Thus, according to the calculations of Chakraborty and Ganguly (1992), the $\log(fO_2)$ in our experiments varied from ~ -13.5 bars at 950°C to ~ -10 bars at 1325°C.

Table 1. Summary of experimental data for Fe^{2+}-Mg diffusion in spinel. D(Fe) and D(Mg) are the self-diffusion coefficients for Fe^{2+} and Mg, respectively.

Run	P (kb) (nominal)	T (°C)	Time (hr)	D(Fe) ($\times 10^{14}$ cm^2/s)	D(Mg) ($\times 10^{14}$ cm^2/s)
Sp-diff07b	19.6	950	381.0	9.8	4.5
Sp-diff04a-03	21.1	1000	338.0	9.0	10.0
Sp-diff02g	20.8	1050	114.0	26.0	25.0
Sp-diff05d	21.4	1125	51.0	60.0	45.0
Sp-diff01a	21.6	1200	48.0	240.0	140.0
Sp-diff06d	22.6	1325	7.2	600.0	500.0
Sp-diff10a	30.0	1125	91.2	4.0	2.0

2.3. Measurement of Diffusion Profiles and Effect of Grain Boundary Diffusion

The compositional change of spinel across the interface of a diffusion couple was determined by a high-resolution beam scanning technique (Chakraborty and Ganguly, 1992; Ganguly et al., 1998a) in a Cameca SX50 electron microprobe. The beam was electronically moved at 0.50- or 0.25-μm steps, depending on the total length of the diffusion zone, along a traverse normal to the interface of the diffusion couple. Each spot was analyzed for Mg, Fe, Al, and Si by wavelength dispersive spectrometry, with 15-kV accelerating voltage and 20-nA beam current. Synthetic end-member enstatite was used as standard for Mg and Si, whereas synthetic end-member hercynite, $FeAl_2O_4$, was used as a standard for Fe and Al. The calibrations for Fe and Si were tested against a secondary standard of synthetic ferrosilite. If 80% of the spot analyses on the primary and secondary standards were within 1.5 mol% of the expected composition, the calibration was used for chemical analyses. Because no Fe^{3+} was detected in the synthetic intermediate spinel by Mössbauer spectroscopy, we assumed that there was no significant Fe^{3+} in the diffusion-annealed samples. This is because the diffusion couples were encased in graphite capsules, as in the synthesis experiments, and the composition across the diffusion zone became progressively more Mg rich from that of the synthetic intermediate spinel, which further enhanced the stability of Fe^{2+} in the samples.

Backscattered electron images of the diffusion couples showed limited effect of grain boundary diffusion within the sintered pellets. As an example, we show in Figure 2 the backscattered electron images of a diffusion couple that was annealed at 21 kb, 1000°C, for 338 h. Figure 3 shows a map of isoconcentration lines in a small area of the diffusion couple illustrated in Figure 2b. This map was prepared by combining the data on a large number of line traverses normal to the interface. The somewhat larger spacing between the isoconcentration lines in some sections of the map is due to the effect of limited grain boundary diffusion. Even then, the retrieved coefficients vary by less than a factor of two within the mapped domain. For other experiments, we avoided this laborious procedure of preparation of concentration maps, but instead measured several diffusion profiles along line traverses in carefully selected areas from backscattered electron images, and modeled the shortest ones to retrieve the volume diffusion coefficients. The traverse lines were chosen to fall within visible single crystals in the sintered pellet. The size of these single crystals were more than 100 μm along the traverse direction, whereas the beam size was smaller than 5 μm. Examples of measured diffusion profiles are shown in Figure 4.

The interface ($x = 0$) between the two components of a diffusion couple can be located by satisfying the condition that the material that diffused out from one side of the interface must be present on the other side. Mathematically, this is given by the condition

$$\int_{C_0}^{C_1} x\,dC = 0, \qquad (1)$$

where C_0 and C_1 are the initial concentrations on two sides of the interface. It is evident from the diffusion profiles shown in Figure 4 that the $x = 0$ position, which is located by satisfying Eqn. 1 (also known as the Boltzmann-Matano interface), lies almost exactly at the middle of the diffusion zone. Consequently, there could be no significant difference between the diffusivities on two sides of the interface along the chosen line traverses. This observation and the fact that we have been able to model the diffusion profiles by constant values of self-diffusion coefficients (see below) rule out any significant interference from grain boundary diffusion in the development of

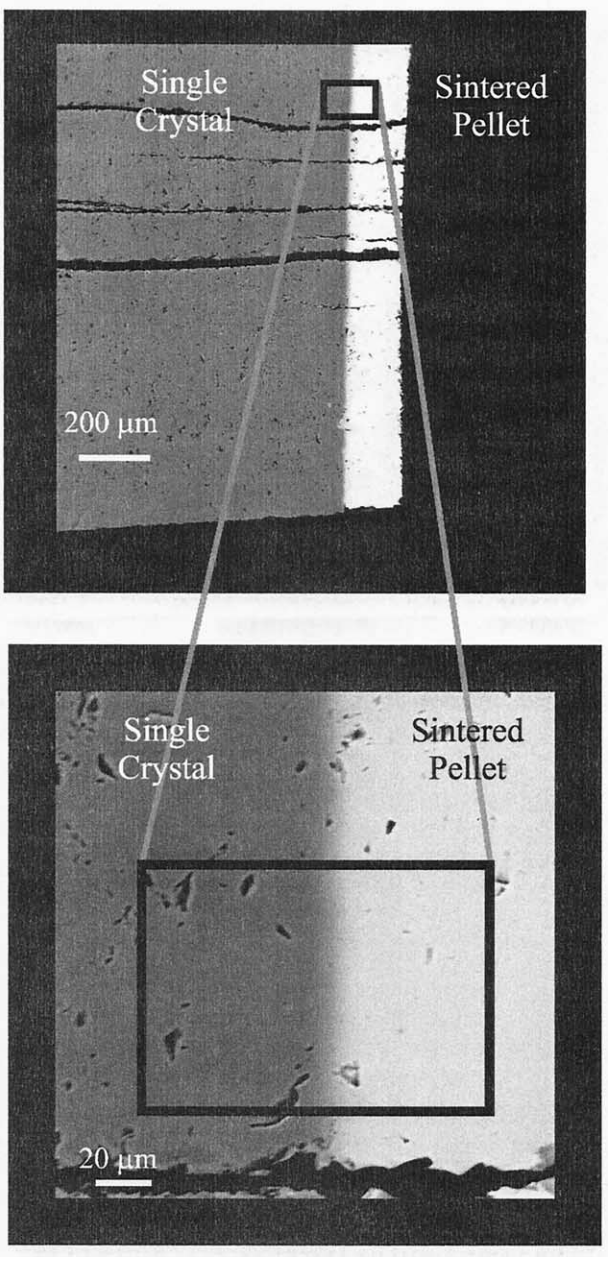

Fig. 2. Backscattered electron images of a diffusion couple consisting of a natural single crystal (nearly pure $MgAl_2O_4$) and synthetic sintered pellet of $(Fe_{0.5}Mg_{0.5})Al_2O_4$. Horizontal cracks in (a) are extension fractures resulting from the release of uniaxial stress after quenching in the piston-cylinder apparatus; (b) enlarged view of the indicated areas in (a). The experimental condition was 21 kb, 1000°C.

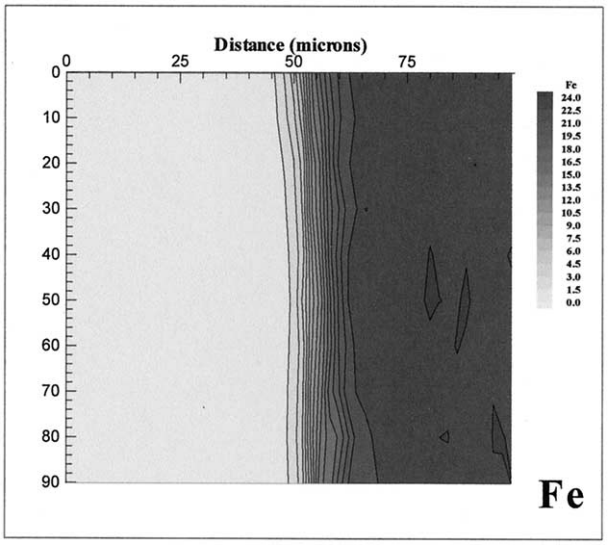

Fig. 3. Concentration map of Fe within the area shown in Figure 2(b). The lines near the interface are isoconcentration contours. The single crystal is on the left side of the interface.

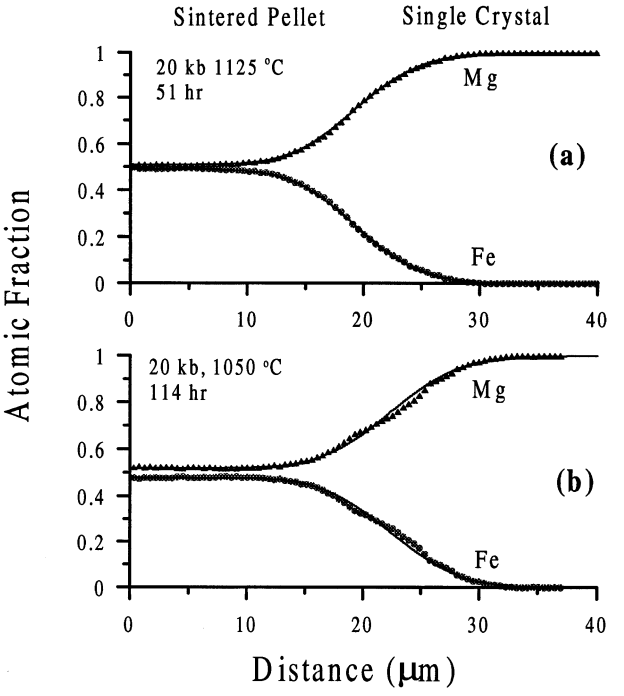

Fig. 4. Examples of experimental diffusion profiles of Fe and Mg, as determined by beam scanning in an electron microprobe normal to the interface of diffusion couples. The couples consist of natural single crystal of nearly pure $MgAl_2O_4$ and synthetic hot-sintered pellet of $(Fe_{0.5}Mg_{0.5})Al_2O_4$. The circles and triangles represent the measured atomic fractions of Fe and Mg, respectively. The solid lines represent the best fit numerical simulations; self-diffusion coefficients were used as inputs. (a) Typical example of numerical simulation of the diffusion profiles. (b) Worst case for the modeling of experimental data.

the profiles that we have selected for the determination of the diffusion coefficients.

3. DETERMINATION OF DIFFUSION PARAMETERS

3.1. Modeling Procedures

In a binary diffusion process, the flux of both components at any point is governed by the same diffusion coefficient, which represents the interdiffusion coefficient of the two components. Consequently, the diffusion equation for either component is given by

$$\frac{\partial C_i}{\partial t} = \frac{\partial}{\partial X}\left(D(i-j)\frac{\partial C_i}{\partial X}\right), \tag{2}$$

where C_i is the concentration of the component i and $D(i-j)$ is the interdiffusion coefficient. In general, $D(i-j)$ is a function of composition. In a semi-infinite diffusion couple, $D(i-j)$ is conventionally retrieved by modeling the measured diffusion profile of either component according to what has been known as the Boltzmann-Matano or simply the Matano analyses (e.g., Buening and Buseck, 1973; Misener, 1974). This procedure yields

$$D(i-j)_{C_1} = -\frac{1}{2t}\frac{dx}{dC}\int_{C_0}^{C_1} x\,dC, \tag{3}$$

where t is the time, $D(i-j)_{C1}$ is the interdiffusion coefficient at a specific composition, C_1, and x is the coordinate axis with the interface located at $x = 0$. However, there is no analytical method to retrieve the self-diffusion coefficients of the diffusing species from the data on $D(i-j)$ as a function of composition.

The interdiffusion coefficient of two equally charged species is related to their self-diffusion coefficients according to (Barrer et al., 1963; Manning, 1968)

$$D(i-j) = \frac{D(i)D(j)}{X_iD(i)+X_jD(j)}\left(1+\frac{\partial \ln\gamma_i}{\partial \ln X_i}\right), \tag{4}$$

where X_i is the atomic fraction of the species i and γ_i is its activity coefficient. The parenthetical term is usually referred to as the thermodynamic factor. As discussed elsewhere (Liermann and Ganguly, 1999; Ganguly et al., 2000), Fe^{2+} and Mg mix nearly ideally in the spinel solid solution. Thus, the thermodynamic factor was set equal to unity. We have used Eqns. 2 and 4 and a finite difference scheme to numerically calculate the self-diffusion coefficients of Fe^{2+} and Mg from the interdiffusion profiles.

The finite difference code is a modified version of that used by Ganguly et al. (1998b) to model diffusion profile in a diffusion couple, including fractionation at the interface. In this scheme, the right-hand side of the diffusion equation (Eqn. 2), which represents the change of flux with distance, was described by calculating the flux gradient within an element (m) from the fluxes of the two neighboring elements ($m+1$ and $m-1$). The left-hand side of Eqn. 2 was described by calculating the change of concentration at the element of interest from the present (n) to the next time step ($n+1$). At each element and time step, D(Fe-Mg) was calculated from Eqn. 4 by means of guessed (input) values of the self-diffusion coefficients of Fe^{2+} and Mg. A nonuniform grid spacing was used to capture greater details within the diffusion zone. The input

Table 2. Comparison of the Fe^{2+}-Mg interdiffusion data, D(Fe-Mg), in spinel calculated from the self-diffusion data obtained from numerical simulation with those determined from Boltzamann-Matano (B-M) analysis.

				D(Fe-Mg × 10^{13}	
Run	P (kb)	T (°C)	X_{Mg}	Self-diffusion	B-M
Sp-diff05d	21.4	1125	0.9	5.81	6.06
			0.8	5.63	5.67
			0.7	5.45	5.48
			0.6	5.29	5.36
Sp-diff10a	30.0	1125	0.9	3.86	3.68
			0.8	3.50	3.27
			0.7	3.20	3.18
			0.6	2.95	3.17

values of self-diffusion coefficients were varied until there was a satisfactory match between the computed and measured diffusion profiles of Fe^{2+} and Mg. The retrieved self-diffusion data are summarized in Table 1.

A typical example of numerical simulation of the diffusion profiles, and the input values of D(Fe) and D(Mg) are shown in Figure 4a. Figure 4b represents the worst fit between the model and experimental diffusion profiles. It is evident from the quality of fits illustrated in these figures that the experimental interdiffusion data were simulated very well by the numerical method described above to retrieve D(Fe) and D(Mg). Also, there was no need to invoke any compositional dependence of the self-diffusion coefficients within the range of compositional variation in the diffusion couples. D(Fe-Mg) may be calculated as a function of composition from the retrieved self-diffusion data according to Eqn. 4.

Table 2 shows a comparison of the D(Fe-Mg) data calculated from Eqn. 4, setting $\gamma_i = 1$, with that calculated from the exact solution according to Boltzmann-Matano analysis (Eqn. 3) for two selected experimental diffusion profiles. (To derive D(Fe-Mg) by Eqn. 3, we have smoothed the diffusion data by fitting polynomial functions and carried out the differential and integral operations by means of these functions.) There is very good agreement between the two sets of results, which attests to the validity of the numerical method used in this work to retrieve self-diffusion coefficients from experimental data on interdiffusion in a binary system. Multicomponent extension of this method have been discussed elsewhere (e.g., Loomis et al., 1985; Chakraborty and Ganguly, 1992).

Because D(Fe-Mg) has a weak compositional dependence (Table 2), we adopted a simple approach to estimate the error standard deviations of the diffusion data. For constant diffusion coefficient, the solution of diffusion equation for the initial and boundary conditions defined for the diffusion couple experiments yields (Crank, 1983)

$$C(X, t) = \frac{C_1 - C_0}{2}\,\mathrm{erfc}\,\frac{X}{2\sqrt{Dt}} \tag{5.1}$$

or

$$\mathrm{erf}^{-1}\left[\frac{C_1 - C_0 - 2C(X, t)}{C_1 - C_0}\right] = \frac{X}{2\sqrt{Dt}}, \tag{5.2}$$

where C_1 and C_0 are the initial concentrations on the two sides of the interface with $C_1 > C_0$. For constant D, the inverse error function vs. X is linear with the slope corresponding to the reciprocal of $2(Dt)^{1/2}$. Thus, the error estimate of the slope yields that of D with the appropriate manipulation, which should be obvious. This exercise for the data from each diffusion couple experiments shows that the standard deviations of D are within a few percent of their reported values. An example of the inverse error function vs. distance plot is shown in Figure 5.

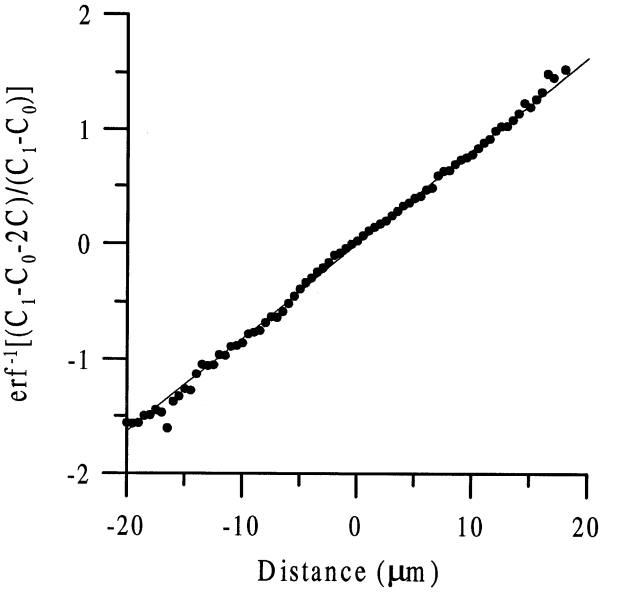

Fig. 5. Inverse error function of a concentration term vs. distance plot of the data from a diffusion couple experiment at 21.6 kb, 1200°C, 48.0 h according to the form of Eqn. 5.2. The interface is located at X = 0. The diffusion coefficient can be calculated from the slope of the regressed line.

3.3. Diffusion Parameters

The retrieved D(Fe) and D(Mg) values as a function of temperature at nominal pressures around 21.2 kb are illustrated in Figure 6 in the form of an Arrhenius plot of logD vs. 1/T. No correction was made for the pressure effect on the diffusion coefficient for the ±1.5 kb pressure variation around the mean nominal pressure in the experimental conditions of these samples. The effect 1.5-kb pressure change on the diffusion coefficient is expected to be negligible compared with the uncertainty of the data. The parameters in Arrhenian relation, $D = D_0 e^{-Q/RT}$, where Q is the activation energy at the average experimental pressure of ~21 kb, were evaluated from the slopes and intercepts of the regressed relations of logD(Fe) vs. 1/T and logD(Mg) vs. 1/T (Fig. 6) and are as follows:

$$\begin{aligned} &\text{Fe: } D_0 = (1.8 \pm 2.8) \times 10^{-5}\ \mathrm{cm^2/s}, \\ &Q = 197.5 \pm 18.8\ \mathrm{kJ/mol} \\ &\text{Mg: } D_0 = (1.9 \pm 1.4) \times 10^{-5}\ \mathrm{cm^2/s}, \\ &Q = 202.1 \pm 7.9\ \mathrm{kJ/mol}, \end{aligned} \tag{6}$$

where the uncertainties represent one standard deviation (1σ).

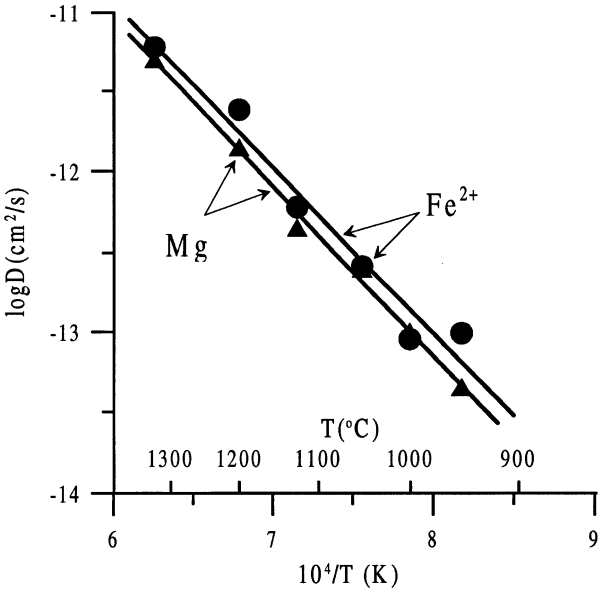

Fig. 6. Arrhenian plot of the self-diffusion data of Fe^{2+} (circles) and Mg (triangles) in spinel at 21.2 (±1.5) kb obtained from diffusion couple experiments at fO_2 defined by graphite capsules. The solid lines are least squares fit to the data.

The uncertainties were evaluated from the relation that if $Z = f(X_1, X_2...)$, then

$$(\sigma_Z)^2 \approx \sum \frac{\partial Z}{\partial X_i}(\sigma_{X_i})^2. \quad (7)$$

The application of this relation to the evaluation of the uncertainty of Q is straightforward. The uncertainties of D_0 from the those of $\log D_0$ (which were obtained from the regression of logD vs. 1/T) were evaluated as follows. If $\log D_0 = X \pm \sigma_X$, then from Eqn. 7 and the relation $\ln D_0 = 2.303X$ so that $dD_0/(D_0 dX) = 2.303$, we have

$$\sigma_{D_0} = \left(\frac{dD_0}{dX}\right)\sigma_X = (2.303D_0)\sigma_X, \quad (8)$$

where $D_0 = 10^X$.

We do not have adequate diffusion data as a function of pressure to determine the activation volume, ΔV^+. However, we have performed two additional experiments, one at 30 kb and 1125°C, and the other at 25 kb and 1125°C. The last experiment was unsuccessful because of excessive fracturing of the sample, but the one at 30 kb yielded smooth diffusion profiles. Comparison of the self-diffusion data obtained from these profiles with those at 20 kb, 1125°C, yields an average $\Delta V^+ \sim 6$ cm^3/mol for Fe and Mg. This activation volume is similar to those measured in garnet (Chakraborty and Ganguly, 1992) and olivine (Misener, 1974), which range between 5.3 and 6.0 cm^3/mol.

As discussed above, the fO_2 in the diffusion couple of experiments was imposed approximately by the graphite-O_2 buffer, which is also a function of P and T. Thus, the data on the temperature and pressure dependence of the diffusion coefficients, which were used to retrieve the above values of Q and ΔV^+, implicitly incorporate the effect of variation of fO_2 along the graphite buffer. However, the fO_2 of this buffer is not sufficiently sensitive to pressure (Chakraborty and Ganguly, 1992) to have any significant effect on the retrieved value of ΔV^+. Assuming that increasing fO_2 enhances the diffusion process, the activation energy of diffusion would decrease, as discussed by Chakraborty and Ganguly (1991), if the diffusion data as function of T along the graphite-O_2 buffer are normalized to those at constant fO_2. The extent by which the Q value would decrease depends on the effect of fO_2 on D. If D varies as $(fO_2)^{1/6}$, as expected from the effect of fO_2 on defect concentration controlled by Fe^{2+}-Fe^{3+} equilibrium in a solid (e.g., Morioka and Nagasawa, 1991), then the Q value would decrease by ~38 kJ/mol (Chakraborty and Ganguly, 1991)

4. COMPARISON WITH OTHER EXPERIMENTAL DIFFUSION DATA

4.1. Diffusion Data in Spinel

Figure 7 shows a comparison of the of D(Fe) and D(Mg) data obtained in this work at ~21 kb with the 1-bar data on D(Mg) and D(Fe-Mg) determined by Sheng et al. (1992) and Freer and O'Reilly (1980), respectively. Because aluminous spinel is nearly an ideal solution of the Fe^{2+} and Mg end members (Liermann and Ganguly, 1999; Ganguly et al., 2000), D(Fe-Mg) must lie, according to Eqn. 4, within the bounds of D(Fe) and D(Mg). Thus, our data are in strong disagreement with those of Freer and O'Reilly (1980). We present below a discussion of their experimental procedure and quality of their diffusion profiles, which would help to evaluate the validity of their diffusion data.

(1) The diffusion couple used by Freer and O'Reilly (1980) consisted of a cube of synthetic hercynite that was pressed into powdered Mg-spinel at a pressure of 420 kg/cm^2 at room temperature. In our experience, this P-T condition is insufficient to produce a tightly sintered pellet with sealed grain boundaries.

(2) In contrast to our polishing procedure, as discussed above, Freer and O'Reilly (1980) polished the mating surfaces of the samples with a 600-grit (40 μm) polishing compound, which is too coarse to produce adequate polishing for diffusion couple experiments.

(3) They annealed the diffusion assemblage in evacuated glass tube, and argued that the fO_2 was controlled by the sample material during their experiments. It is, however, not clear what that fO_2 value was.

(4) In contrast to the smooth and nearly symmetric diffusion profiles (with respect to the interface) obtained in our work (Fig. 4), the diffusion profiles obtained by the Freer and O'Reilly (1980) had complex shapes. Indeed, the shapes are much more complex than those encountered in recent studies of Fe-Mg interdiffusion in garnet (Chakraborty and Ganguly, 1992; Ganguly et al., 1998a) and olivine (Chakraborty, 1997; Meissner et al., 1998). The complexity of diffusion profiles obtained by Freer and O'Reilly (1980) implies strong influence of the Fe^{2+}/Mg ratio on D(Fe) and D(Mg), which is difficult to reconcile with the fact that Fe^{2+} and Mg mix nearly ideally in spinel.

On the basis of the above observations, we conclude that the diffusion profiles modeled by Freer and O'Reilly (1980) were marred by interference from grain boundary diffusion in the

polycrystalline samples, and the effects from surface irregularities and fO_2, which was undefined. The potential effects of grain boundary diffusion were also recognized by these workers.

The D(Mg) data obtained in our study at ~21 kb is slightly smaller than that obtained by Sheng et al. (1992) at 1 bar within the small overlapping temperature range around 1325°C (Fig. 6). Correction for the pressure effect according to $\Delta V^+ = 5$ cm^3/mol, as deduced above, increases the logD(Mg) value in our study by 0.39, which brings our data in almost perfect agreement with that value obtained by Sheng et al. (1992). In principle, the difference between the activation energies (which is reflected in the difference between the slopes in the Arrhenian plot) between the two sets of data could be due to one of the following reasons: (1) a change from grain boundary diffusion at low temperature to volume diffusion at high temperature (e.g., Shewmon, 1963); however, this explanation can be convincingly ruled out on the basis of arguments presented in section 2.3; (2) Difference between the compositions of the samples used by Sheng et al. (1992) and in this work; and (3) a change of volume diffusion mechanism as a function of temperature (low temperature extrinsic to high temperature intrinsic mechanism; e.g., Shewmon, 1963) at ~1200°C.

Chakraborty et al. (1994) found that the activation energy for Mg self-diffusion in nominally pure synthetic forsterite (Fo_{100}) at 1000 −1300°C is 400 (±60) kJ/mol as compared with that of 275 (±25) kJ/mol in San Carlos olivine (Fo_{92}) within the same temperature range. Both sets of experiments were carried out by them following the same experimental technique. Also the D(Mg) in the San Carlos olivine had a much stronger fO_2 dependence than that in Fo_{100} (the latter was found to be quite weak). Chakraborty et al. (1994) thus suggested that the diffusion mechanism in the nominally pure forsterite is different from that in olivine, which contains significant amount of Fe^{2+}. When the FeO content falls below a critical value, the vacancies created by the Fe^{2+}-Fe^{3+} equilibria have relatively minor role in the diffusion process. In the light of these results, it seems quite likely that the high activation energy (343 ±25 kJ/mol) of Mg self-diffusion in the studies of Sheng et al. relative to that in ours (202 ± 8 kJ/mol) is due to the extremely small (probably below the detection limit in microprobe analysis) FeO content in their sample (they did not report any FeO in their microprobe analysis of the sample, for which the wt% MgO, Al_2O_3, SiO_2, and CaO add up to 100.88).

The third option cannot be ruled out and needs to be tested with more experimental data in the Fe-Mg system at temperatures above 1300°C. However, these are difficult conditions for successful diffusion couple experiments in the piston-cylinder apparatus because of the high probability of thermocouple failure and fracturing of the pressure cores. These high-temperature experiments have therefore been postponed to future studies. We note in the meanwhile that there has not been any convincing demonstration of the change of diffusion mechanism in mineralogical systems. (See, for example, Dimanov et al., 1996; Chakraborty, 1997; Ganguly et al., 1998a; Meissner et al., 1998; in the first reference, the authors have chosen to show a change of mechanism for Ca diffusion in diopside, but considering their scatter, one can fit the experimental data by a single Arrhenian relation.)

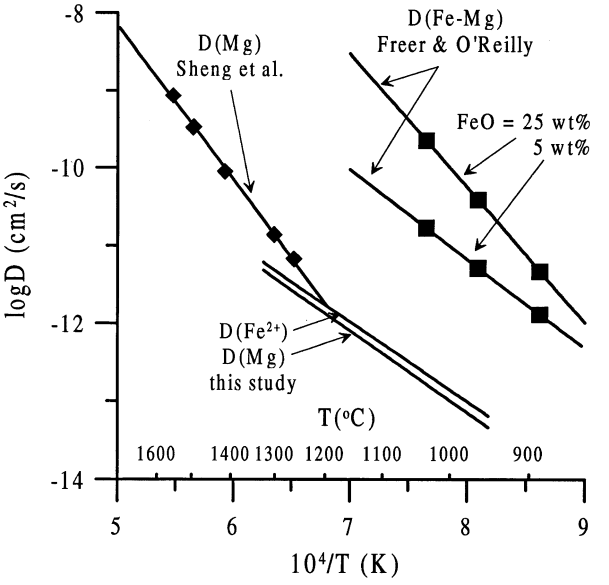

Fig. 7. Comparison of the D(Fe) and D(Mg) data in spinel determined in this work at ~20 kb with D(Mg) in spinel determined by Sheng et al. (1992), and D(Fe-Mg) in spinel determined by Freer and O'Reilly (1980) at two different compositions. The last two sets of data at 1 bar. The symbols represent the experimental data.

4.2. Diffusion Data in Olivine and Implications

Buening and Buseck (1973) and Misener (1974) determined D(Fe-Mg) in olivine at 1000 to 1200°C, and 900 to 1100°C, respectively. Their data for diffusion parallel to the c-axis are illustrated in Figure 8 for an olivine composition of Fo_{86}, as calculated by Chakraborty (1997) by using the Arrhenian relations given by these authors. However, as he emphasized, calculation of Fe-Mg interdiffusion in olivine that uses Misener's Arrhenian relation should be restricted to its stated domain of validity of $0.1 \leq X_{Mg} \leq 0.8$ This particular composition of Fo_{86} was chosen by Chakraborty (1997) for comparison with his data, which are discussed below.

Diffusion in olivine is anisotropic with $D_{\|c} > D_{\|a} > D_{\|b}$, and $D_{\|c}$ probably around a factor of 15 larger than $D_{\|b}$ (Misener, 1974). The data of Buening and Buseck (1973), which have been used extensively in the literature to constrain the thermal histories of both terrestrial and planetary samples, show a change of activation energy at ~1100 to 1130°C. They suggested change from the high temperature intrinsic to the low-temperature extrinsic diffusion mechanism as a possible explanation for the change of activation energy. As evident from Figure 7, the Arrhenian relation given by Misener (1974) for the temperature range 900 to 1100°C corresponds to an activation energy that is similar to that given by Bunening and Buseck (1973; Fig. 8) at higher temperature (i.e., above the temperature of the supposed change of diffusion mechanism). These results are, however, in sharp contrast to those of Chakraborty (1997). The latter was confirmed by the measurement of diffusion profiles in olivine/olivine diffusion couples in an analytical transmission microscope by Meissner et al. (1998). (However, as discussed by Chakraborty, 1997, Misener's [1974] experimental results for more Mg-rich composition,

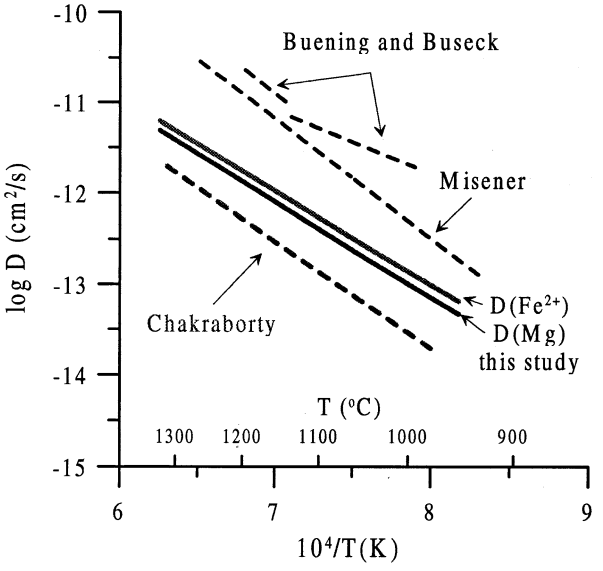

Fig. 8. Comparison of the self-diffusion data of Fe^{2+} and Mg in spinel (solid lines) determined in this work with the D(Fe-Mg) data parallel to the c-axis for olivine (Fo_{86}), as determined by Buening and Buseck (1973), Misener (1974), and Chakraborty (1997). The olivine data are shown by dashed lines. Considering the observation of Ozawa (1984) on the relative D(Fe-Mg) values in spinel and olivine, only the D(Fe-Mg) data in olivine by Chakraborty (1997) are compatible with our diffusion data in spinel.

$\geq Fo_{93}$, are consistent with his data, which led him to suggest that Meisener's data for $0.1 \leq X_{Mg} \leq 0.8$ were somehow marred by the poor fO_2 control.)

From analysis of compositional gradients in coexisting olivine and spinel in ultramafic rocks, Ozawa (1984) concluded that D(Fe-Mg) in spinel with $Cr/(Cr + Al) \leq 0.5$ is ~100 times larger than that in olivine ($\sim Fo_{90}$). Using the Fe-Mg diffusion data in spinel obtained in this work, Ozawa's constraint is satisfied only by the olivine diffusion data of Chakraborty (1997). Thus, there is a strong independent reason to accept the data of Chakraborty (1997) and reject those of Buening and Buseck (1973) and Misener (1974).

5. APPLICATIONS

The Fe^{2+}-Mg diffusion data in spinel can be applied to both terrestrial and meteorite samples to derive constraints on their thermal histories on the basis of diffusion induced/modified compositional zoning in spinels (e.g., Ozawa, 1984; Liermann and Ganguly, 2001). However, both terrestrial and meteoritic spinels often have significant concentration of Cr. In addition, the terrestrial samples may also have significant concentration of Fe^{3+}. Therefore, proper modeling of compositional zoning in spinels should await the availability of experimental data on the effect of these trivalent cations on Fe-Mg interdiffusion in spinel, except in those special cases where the concentration of these components is dilute (e.g., Liermann and Ganguly, 2001). In addition, Fe-Mg interdiffusion in spinel is expected to depend also on fO_2. We discuss below some first-order observations on the cooling rates of selected meteoritic and terrestrial samples on the basis of their compositional heterogeneity.

5.1. Mg Isotopic Heterogeneity in POIs in Allende Meteorite

Sheng et al. (1991) found surprising variations of Mg isotopic composition of up to 11‰/amu between spinel and the coexisting silicates of the POIs in the Allende meteorite, despite textural evidence of molten or partially molten origin. Thus, they proposed that the POIs had formed by the partial melting of an isotopically heterogeneous aggregate. Even within a single inclusion, the spinel grains showed considerable (up to 7‰/amu) Mg isotopic variation. According to Sheng et al. (1992), "most spinel grains in POIs are less than 10 μm across." By using this limiting grain size and their D(Mg) data of spinel, Sheng et al. (1992) concluded that to preserve the isotopic heterogeneity, the initial cooling rate (Γ_0) of the POIs must have been >100°C/h, for a suggested maximum temperature ~1500°C. Consequently, the nature of heating process must have been short, such as flash heating or impact melting, so that there was rapid cooling. Although it does not affect their qualitative conclusion, Sheng et al. (1992) noted that their Γ_0 value is substantially higher than that inferred from petrographic studies, which suggest Γ_0 between a few tenths and 50°C/h. Thus, they preferred a lower initial temperature (T_0), ~1350°C, in order that their results on cooling rates agree with the petrographic observations.

In stating the minimum cooling rate at 1500°C, Sheng et al. (1992) seem to have inadvertently substituted the diameter, instead of the radius, of the grain for the characteristic diffusion distance, χ. (Otherwise, their estimate of minimum cooling rate required to preserve Mg isotopic heterogeneity in grains that are 10 μm across does not follow from their Fig. 9.) Correcting for this problem yields $\Gamma_o > 400$°C/h. Furthermore, they estimated Γ_0 by equating the square of radial dimension of spinel (i.e., χ^2) with $\int_0^\infty D(t)dt$, referred to as $\tau(\infty)$, and evaluating this integral from the diffusion data. However, $\chi^2 = \alpha\tau(\infty)$, with the value of α, which is >1, depending on the initial and boundary conditions governing the diffusion process. For random walk diffusion, $\alpha = 2$. It can be shown (Ganguly et al., 1994) that for given values of χ, T_0, and diffusion parameters, the cooling rate varies as α. Therefore, the discrepancy with the petrographic cooling rate is much larger than that noted by Sheng et al. (1992). It is, however, interesting to note that this discrepancy essentially vanishes if our diffusion data are extrapolated to higher temperature, which yields Γ_0 ~10 to 40°C/h for T_0 = 1350 to 1500°C, and $\alpha = 1$. As discussed above, it is possible that the diffusion data of Sheng et al. (1992) in essentially pure $MgAl_2O_4$ may not be applicable to the spinels in Allende that have variable contents of FeO (0.95 to 8.87 wt%), Cr_2O_3 (0.59 to 9.76 wt%), V_2O_3 (0.09 to 0.69 wt%), and TiO_2 (0.19 to 2.94 wt%) (Sheng et al., 1991). On the other hand, the additional components may have significant effect on Mg diffusion in spinel leading to a significant change in the inferred cooling rate of the POIs on the basis of diffusion data in the ferromagnesian system and fO_2 defined by graphite buffer.

5.2. Cooling Rates of Terrestrial Ultramafic Rocks

Ozawa (1984) carried out elaborate finite difference modeling of the evolution of compositional zoning in olivine and spinel as function of cooling rate, and presented useful graphs

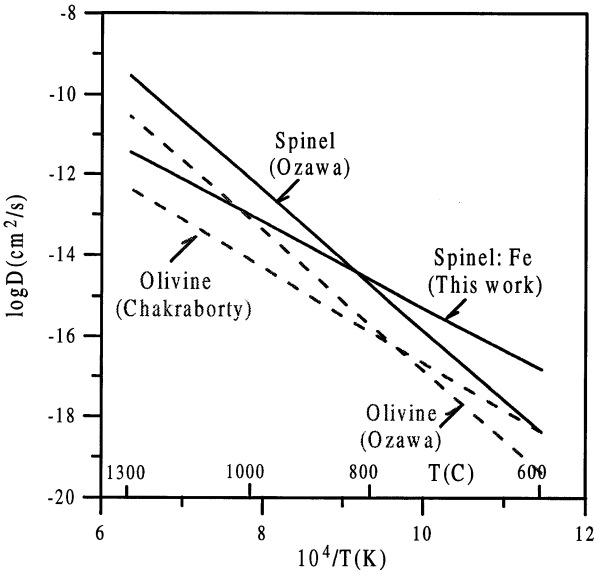

Fig. 9. Comparison of D(Fe-Mg) in spinel and olivine ($\sim Fo_{90}$), which were used by Ozawa (1984) for calculation of cooling rates of olivine-spinel pairs (Cr/(Cr + Al) in spinel ≤ 0.5) in ultramafic rocks, with those determined in this work for spinel and by Chakraborty (1997) for olivine (Fo_{86}). Solid lines = diffusion data for spinel; dashed lines = diffusion data for olivine. For the data from this work, only D(Fe) for spinel is shown because both D(Fe) and D(Mg) values are very close to one another (see Fig. 5), and D(Fe-Mg) for Mg-rich compositions are closer to D(Fe) than to D(Mg), according to Eqn. 4. The semiempirical olivine D(Fe-Mg) data of Ozawa is for diffusion parallel to the a-axis. The $D(Fe\text{-}Mg)_{\|a}$ of Chakraborty (1997) was derived from $D(Fe\text{-}Mg)_{\|c}$ using the relation $D_{\|c} \sim 4 \times D_{\|a}$, according to Chakraborty et al. (1994).

relating cooling rates to initial temperatures (1200 to 1300°C), grain size and closure temperatures of Fe-Mg diffusion in olivine-spinel pairs. He also applied these graphs to estimate the cooling rates of a number of terrestrial ultramafic rocks. Ozawa found that the diffusion data in olivine by Buening and Buseck (1973) and Misener (1974) led to "unreasonably large cooling rates for peridoties and ophiolite complexes." This observation implies that the D(Fe-Mg) data for olivine by the above workers are unusually large and is thus consistent with our conclusion about these data. By using a combination of experimental and observational data (Wilson, 1982), Ozawa (1984) developed an Arrhenius expression for Fe-Mg interdiffusion parallel to a-axis in Mg-rich olivine as $D(Fe\text{-}Mg) = 3.0 \exp(-Q/RT)$ cm^2/s, where $Q = 332$ kJ/mol. From the diffusion zoning in natural spinel–olivine pairs, he also concluded that the D value in spinels with $Cr/(Cr + Al) \leq 0.5$ is approximately 100 times larger than that in olivine, and that at higher Cr content D(Fe-Mg) in spinel becomes smaller.

Figure 9 shows a comparison of the semiempirical diffusion data for olivine and spinel used by Ozawa (1984) with the preferred olivine diffusion data from Chakraborty (1997) and the spinel diffusion data as determined in this work. Ozawa's D(Fe-Mg) data for olivine applies to diffusion parallel to the a-axis, whereas the experimental data of Chakraborty (1997) are for diffusion parallel to the c-axis. However, according to Chakraborty et al. (1994), $D_{\|c} \sim 4 \times D_{\|a}$. This correction was applied to derive $D(Fe\text{-}Mg)_{\|a}$ from $D(Fe\text{-}Mg)_{\|c}$ of Chakraborty (1997). As evident from Fig. 9, Ozawa's semiempirical data are quite similar to the experimental data at 800 to 900°C, but larger at higher temperature and lower at lower temperature. Because D value has an exponential dependence on T, the discrepancy at higher temperature is more significant for rocks with initial temperatures of 1200 to 1300°C that were used by Ozawa.

Numerical simulations by Ozawa (1984) suggest that the inferred cooling rate is relatively insensitive to the changes of diffusion data in spinel. Thus, if D(Fe-Mg) in spinel is increased by a factor of 100, the cooling rates increase only by a factor of two. This is because of the fact that the mineral with slower diffusion property (in this case olivine) has greater control on the development of compositional profiles in a composite diffusion couple. Thus, the difference between the D(Fe-Mg) values determined in this work and those used by Ozawa (1984) will have a relatively small effect on the inferred cooling rate. (However, the difference could be larger after the experimental D values are corrected for the effect of Cr.) More significant is the difference between the D(Fe-Mg) data in olivine. A rough estimate of the effect of the change of the diffusion coefficient may be made by noting that the characteristic diffusion distance during cooling scales as $D(T_0)/Q$ (Sheng et al. 1992; Ganguly et al., 1994). By use of this approach, the cooling rates of rocks with initial temperatures of 1200 and 1300°C and $X_{Cr}(spinel) \leq 0.5$ seem to have been overestimated by $\sim$80 and $\sim$240 times, respectively.

Acknowledgments—We are grateful to Prof. Hans Annersten for the Mössbauer spectroscopy of synthetic spinel samples, Prof. Robert Downs for his help in the single crystal X-ray diffraction studies, and Dr. Andy Freed for making available to us his finite difference code for modeling diffusion profiles. Constructive reviews by Prof. Sumit Chakraborty, Prof. Richard Yund, and an anonymous reviewer have led to substantial improvements. This research was supported by NASA grants NAG5-7364 and NAG5-10486.

Associate editor: M. S. Ghiorso

REFERENCES

Barrer R. M., Bartholomew R. F., and Rees L. V. C. (1963) Ion exchange in porous crystal, part II: The relationship between self- and exchange diffusion coefficients. *J. Phys. Chem. Solids* **24,** 309–317.

Bose K. and Ganguly J. (1995) Quartz–coesite transition revisited: Reversed experimental determination at 500–1200°C and retrieved thermochemical properties. *Am. Mineral* **80,** 231–238.

Buening D. K. and Buseck P. R. (1973) Fe-Mg lattice diffusion in olivine. *J. Geophys. Res* **78,** 6852–6862.

Chakraborty S. (1997) Rates and mechanisms of Fe-Mg interdiffusion in olivine at 980–1300°C. *J. Geophys. Res* **102,** 12317–12331.

Chakraborty S. and Ganguly J. (1991) Compositional zoning and Cation Diffusion in Garnet. In *Diffusion, Atomic Ordering, and Mass Transport: Advances in Physical Geochemistry,*, Vol. 9 (ed. J. Ganguly), pp. 120–175. Springer-Verlag, New York.

Chakraborty S. and Ganguly J. (1992) Cation diffusion in aluminosilicate garnets: Experimental determination in spessartine–almandine diffusion couples, evaluation of effective binary diffusion coefficients, and applications. *Contrib. Mineral. Petrol* **111,** 74–86.

Chakraborty S., Farver J. R., Yund R. A., and Rubie D. C. (1994) Mg tracer diffusion in synthetic forsterite and San Carlos olivine as a function of P, T and fO_2. *Contrib. Mineral. Petrol* **21,** 489–500.

Chakraborty S. and Rubie D. C. (1996) Mg tracer diffusion in aluminosilicate garnets at 750–850°C, 1 atm, and 1300°C, 8.5 GPa. *Contrib. Mineral. Petrol* **122,** 406–414.

Crank J. (1983) *The Mathematics of Diffusion*. Clarendon Press, Oxford, UK.

Dimanov A., Jaoul O., and Sautter V. (1996) Calcium self-diffusion in natural diopside single crystals. *Geochim. Cosmochim. Acta* **60,** 4095–4106.

Elphick S. C., Ganguly J., and Loomis T. P. (1985) Experimental determination of cation diffusivities in aluminosilicate garnets. I. Experimental methods and interdiffusion data. *Contrib. Mineral. Petrol* **90,** 36–44.

Freer R. and O'Reilly W. (1980) The diffusion of Fe^{2+} ions in spinel with relevance to the process of maghemitization. *Mineral Mag* **43,** 889–899.

Ganguly J., Cheng W., and Chakraborty S. (1998a) Cation diffusion in aluminosilicate garnets: Experimental determination in pyrope–almandine diffusion couples. *Contrib. Mineral. Petrol* **131,** 171–180.

Ganguly J., Cheng W., and Freed A. (1998b) Modeling bi-mineral diffusion couples in experimental and natural samples. *Terra Nova Abstracts* **10,** (Suppl 1) 18.

Ganguly J., Yang H., and Ghose S. (1994) Thermal history of mesosiderites: Quantitative constrains from compositional zoning and Fe-Mg ordering in orthopyroxenes. *Geochim. Cosmochim. Acta* **58,** 2711–2723.

Ganguly J., Dasgupta S., Cheng W., and Neogi S. (2000) Exhumation history of a section of the Sikkim Himalayas, India: Records in the metamorphic mineral equilibria and compositional zoning of garnet. *Earth Planet. Sci. Lett* **183,** 471–486.

Hermeling J. and Schmalzried H. (1984) Tracer diffusion of the Fe-cations in olivine $(Fe_xMg_{1-x})_2SiO_4$. *Phys. Chem. Miner* **11,** 161–166.

Lane D. L. and Ganguly J. (1980) Al_2O_3 solubility in orthopyroxene in the system $MgO\text{-}Al_2O_3\text{-}SiO_2$: A Reevaluation, and Mantle Geotherm. *J. Geophys. Res* **85,** 6963–6972.

Liermann H. P. and Ganguly J. (1999) Thermodynamics and kinetics of Fe-Mg exchange between spinel and orthopyroxene: Experimental determination and applications to cooling rates. *62nd Annual Meet. Meteor Soc., Meteoritics & Planet. Sci. Sup* **34,** (Suppl) A75.

Liermann H. P. and Ganguly J. (2001) Compositional properties of coexisting orthopyroxene and spinel in some Antarctic diogenites: Implications for thermal history. *Meteor. Planet. Sci* **36,** 155–166.

Loomis T. L., Ganguly J., and Elphick S. C. (1985) Experimental determination of cation diffusivities in aluminosilicate garnets. I. Multicomponent simulations and tracer diffusion coefficients. *Contrib. Mineral. Petrol* **90,** 45–51.

Manning J. R. (1968) *Diffusion Kinetics for Atoms in Crystals*. Van Nostrand, Princeton, USA.

Meissner E., Sharp T. G., and Chakraborty S. (1998) Quantitative measurements of short compositional profiles using analytical transmission electron microscopy. *Am. Mineral* **83,** 546–552.

Misener D. J. (1974) Cationic diffusion in olivine to 1400°C and 35 kbar. *Geochemical transport and kinetics* In: (eds. W. Hofmann, B. J. Giletti, H. S. Yoder Jr., and R. A. Yund), pp. 117–129. Carnegie Institution Washington, Washington DC.

Morioka M. and Nagasawa H. (1991) Ionic diffusion in olivine. In *Diffusion, Atomic Ordering, and Mass Transport: Advances in Physical Geochemistry*,, Vol. 9 (ed. J. Ganguly), pp. 176–197. Springer-Verlag.

Nakamura A. and Schmalzried H. (1984) On the Fe^{2+}-Mg^{2+} interdiffusion in olivine (II). *Ber. Bunsenges. Phys. Chem* **88,** 140–145.

Ozawa K. (1984) Olivine–spinel geospeedometry: Analysis of diffusion-controlled Mg-Fe^{2+} exchange. *Geochim. Cosmochim. Acta* **48,** 2597–2611.

Redfern S. A. T., Harrison R. J., O'Neill H. St. C., and Wood D. R. R. (1999) Thermodynamics and kinetics of cation ordering in $MgAl_2O_4$ spinel up to 1600°C from in situ neutron diffraction. *Am. Mineral* **84,** 299–310.

Sheng Y. J., Hutcheon I. D., and Wasserburg G. J. (1991) Origin of plagioclase–olivine inclusions in carbonaceous chondrites. *Geochim. Cosmochim. Acta* **55,** 581–599.

Sheng Y. J., Wasserburg G. J., and Hutcheon I. D. (1992) Self-diffusion of magnesium in spinel and in equilibrium melts: Constraints on flash heating of silicates. *Geochim. Cosmochim. Acta* **56,** 2535–2546.

Shewmon P. G. (1963) *Diffusion in Solids*. McGraw-Hill, New York, USA.

Wilson A. H. (1982) The geology of the Great "Dyke," Zimbabwe: The ultramafic rocks. *J. Petrol* **23,** 249–292.